

CustomVideoX: 3D Reference Attention Driven Dynamic Adaptation for Zero-Shot Customized Video Diffusion Transformers

D. She^{*1} Mushui Liu^{*2} Jingxuan Pang² Jin Wang¹ Zhen Yang³ Wanggui He Guanhao Zhang Yi Wang²
 Qihan Huang² H. Tang¹ Yunlong Yu^{†2} Siming Fu^{†2}
 Project Page

(a) Natural motions

Prompt: In a sunlit living room, a playful **cat** chases a colorful yarn ball. Sunlight streams through the windows, casting vibrant shadows on the floor.....



Prompt: In a cozy indoor setting, a **cartoon character** walks slowly, surrounded by colorful toys and books.....



Prompt: In a park, a **dog** gracefully walks forward with steady steps and its tail gently wagging.....



Prompt: A **monster plushie** waves its arms on a wooden table, its lively movements illuminated by the dim yellow light.....



(b) High textual preservation

Prompt: In the morning restaurant, sunlight streams through the window onto the wooden table. A **owl** sits quietly on the table, filled with fresh oatmeal.....



Prompt: Under the bright sunlight, a man wearing a **T-shirt** leisurely walks along the sidewalk. Lined with lush green trees, blooming flowers adorn the streetside flower



(c) Text consistency

Prompt: On a sunny lake surface, a **yellow rubber duck** toy floats peacefully. Surrounding blooming lotus flowers.....



Prompt: In clear lake water, a **dog** joyfully swims. Sunlight glimmers on the sparkling surface, reflecting its wet fur



Prompt: On a bright sunny day, a **horse** walks slowly along the riverbank. Sunlight glimmers on its flowing mane, and the river sparkles with shimmering light.....



Prompt: Under the soft afternoon sunlight, on light brown flooring, a **toy car** glides cheerfully, its wheels producing a faint rustling sound.....



Figure 1: CustomVideoX synthesizes natural motions while preserving the fine-grained object details.

Abstract

Customized generation has achieved significant progress in image synthesis, yet personalized video generation remains challenging due to temporal inconsistencies and quality degradation. In this paper, we introduce CustomVideoX, an innovative framework leveraging the video diffu-

sion transformer for personalized video generation from a reference image. CustomVideoX capitalizes on pre-trained video networks by exclusively training the LoRA parameters to extract reference features, ensuring both efficiency and adaptability. To facilitate seamless interaction between the reference image and video content, we propose 3D Reference Attention, which enables direct and simultaneous engagement of reference image features with all video frames across spatial and temporal dimensions. To mitigate the excessive influence of reference image features and textual guidance on generated video content during inference, we implement the Time-Aware

^{*}Equal contribution ¹University of Science and Technology of China ²Zhejiang University ³Hong Kong University of Science and Technology (Guangzhou). Correspondence to: Siming Fu <fusiming@zju.edu.cn>, Yunlong Yu <yuyunlong@zju.edu.cn>.

Reference Attention Bias (TAB) strategy, dynamically modulating reference bias over different time steps. Additionally, we introduce the Entity Region-Aware Enhancement (ERAE) module, aligning highly activated regions of key entity tokens with reference feature injection by adjusting attention bias. To thoroughly evaluate personalized video generation, we establish a new benchmark, VideoBench, comprising over 50 objects and 100 prompts for extensive assessment. Experimental results show that CustomVideoX significantly outperforms existing methods in terms of video consistency and quality.

1. Introduction

Text-to-video (T2V) generation (Wu et al., 2023; Guo et al., 2024; Yang et al., 2024) have recently garnered extensive attention in the fields of computer vision. The ability to generate visual content from textual descriptions holds significant promise for applications, *e.g.*, digital art creation, and advertising. In this domain, customized video generation (Wei et al., 2024a; Chefer et al., 2024; Jiang et al., 2024; Wu et al., 2024a) aims to generate videos that not only adhere to textual instructions but also maintain consistency with provided reference images. Although strongly in need, this topic remains underexplored unlike customized image generation (Ruiz et al., 2023; Gal et al., 2023; Ye et al., 2023; Chen et al., 2023; Wang et al., 2024; Tan et al., 2024).

Existing work on customized video generation (Wei et al., 2024a;b; Jiang et al., 2024; Wu et al., 2024b;a) still struggles to maintain the subject identity of reference images across varying frames with high fidelity, often overlooking significant detail information. Additionally, the temporal coherence between consecutive frames remains unsatisfactory (Chefer et al., 2024; Wei et al., 2024a), exhibiting discontinuities. These limitations stem from the dual flaws of current frameworks: (1) inefficient exploitation of pixel-level reference guidance during spatial feature encoding, which undermines identity preservation by neglecting local structural cues, and (2) the uniform propagation of reference features throughout the denoising process fails to accommodate the distinct requirements of early-stage structural establishment versus late-stage motion dynamics refinement. This inflexible paradigm results in both identity degradation and temporal coherence artifacts, highlighting the need for temporally-aware reference adaptation mechanisms.

To address the above challenges, we propose *CustomVideoX*, a novel framework for zero-shot personalized video generation grounded in the Video Diffusion Transformer (VDiT) architecture, *e.g.*, CogVideoX (Yang et al., 2024). First,

we develop a 3D Reference Attention mechanism that enables direct interaction between reference image features and each frame of the video within the VDIT framework. This strategy streamlines the interaction process by eliminating the need for separate temporal and spatial attention stages, thereby enhancing both efficiency and effectiveness. The reference image features are extracted using the same VDIT model, obviating the need for additional encoders and ensuring seamless integration. Second, we introduce a Time-Aware Attention Bias mechanism to modulate the influence of reference image features throughout the denoising process inherent in diffusion models. By dynamically modulating the weight of reference image features—initiating with minimal influence when the input predominantly consists of random noise, escalating during intermediate phases, and diminishing in the final stages. This dynamic weighting promotes better temporal coherence and visual quality in the generated videos, allowing the model to capture both the overall structure and fine-grained temporal details effectively. Finally, we introduce an Entity Region-Aware Enhancement (ERAE) module that adaptively focuses on the key entity regions. After computing the attention score of the key entity’s textual token with the latent, we adjust the attention bias by setting a threshold to refine the focus.

To tackle the challenge of limited paired reference video data, we introduce a method for synthesizing high-quality reference video pairs, creating a large-scale dataset of two million (2M) pairs. This enhances training and improves model generalization. We also propose a comprehensive benchmark for personalized video generation, covering a wide range of objects and scenes. As shown in Figure 1, our approach demonstrates strong personalization capabilities. Extensive experiments confirm that our method outperforms existing approaches in video quality and temporal coherence, setting a new state-of-the-art on both existing and proposed benchmarks. The contributions of this paper can be summarized as follows:

- We present CustomVideoX, a zero-shot personalized video generation framework based on the VDIT architecture, enabling physically consistent articulations without compromising high-resolution morphological details.
- The integration of 3D Reference Attention and Time-Aware Attention Bias within CustomVideoX facilitates a more effective learning process between reference images and video generation, resulting in high-quality customized videos.
- We developed a robust data generation pipeline and established a comprehensive evaluation benchmark, demonstrating that CustomVideoX achieves the best video generation performance on both existing and

newly introduced benchmarks.

2. Related Works

Text-to-Video Diffusion Models. The ongoing advancements in diffusion models (Rombach et al., 2022) and text-to-image (T2I) generation models (Betker et al., 2023; Esser et al., 2024; Podell et al., 2023; He et al., 2025; Liu et al., 2024; Ying et al., 2024; Zhao et al., 2024; Sun et al., 2024) have spurred new research initiatives in the realm of text-to-video (T2V) generation models (Guo et al., 2024; Wu et al., 2023). Current studies in video generation predominantly fall into two categories: extending T2I models to T2V models and training T2V generation models directly from scratch. The former prominent works such as AnimateDiff (Guo et al., 2024) and Tune-A-Video (Wu et al., 2023) have emerged. Owing to the limited availability of high-quality video-text paired datasets, these models capitalize on the rich prior knowledge embedded in existing image generation models to synthesize video content. By adapting T2I frameworks, they generate coherent video sequences conditioned on textual input, effectively compensating for the scarcity of video data. In the second category, there is a growing momentum in constructing T2V models directly. For instance, the Video Diffusion Model (VDM) (Ho et al., 2022) extends the capabilities of stable diffusion (Rombach et al., 2022) by incorporating temporal attention mechanisms and 3D-Conv modules to process video data effectively. With the introduction of the Diffusion Transformer (DiT) (Peebles & Xie, 2023), T2V generation models such as Sora and CogVideoX (Yang et al., 2024) have been developed based on the DiT architecture. Notably, CogVideoX employs a 3D-VAE to encode video information, enhancing the model’s ability to capture complex spatiotemporal relationships. Overall, video generation models provide robust technical support for the creation of customized video content and represent a significant research direction in the fields of computer vision and pattern recognition.

Custom Video Generation. Customized video generation aims to produce video content that closely aligns with a given reference image and textual description by integrating both inputs. Prior methods in customized image generation (Ye et al., 2023; Zhang et al., 2024; Wang et al., 2024) primarily fall into two categories: fine-tuning and zero-shot approaches. Fine-tuning methods, exemplified by DreamBooth (Ruiz et al., 2023), achieve high-fidelity generation of specific images through personalized adjustments to pre-trained models. Zero-shot methods, such as IP-Adapter (Ye et al., 2023) and SubjectDiffusion (Ma et al., 2024), incorporate novel concepts or styles into the generation process without additional model training. In the realm of customized video generation, these methodologies have been extended along similar lines. Fine-tuning approaches, including models like Still-Moving (Chefer et al., 2024) and

DreamVideo (Wei et al., 2024a), accomplish customized video generation by specifically tuning video generation models. More recently, zero-shot methods like VideoBooth (Jiang et al., 2024) have showcased the potential for customized video generation without extra training by extending text-to-image (T2I) models (Wu et al., 2023; Yang et al., 2024) to text-to-video (T2V) generation. Different from these works, we explore a zero-shot customized video generation framework based on DiT (Peebles & Xie, 2023) and introduce a novel adaptive feature injection method.

3. Preliminary

Diffusion Models for Text-to-Video Generation. Diffusion models generate samples from Gaussian random noise through multiple sequential denoising steps. These steps form a Markov process that progressively transforms the initial noise x_T into the target sample x_0 , defined as:

$$x_t = \alpha_t x_0 + \sigma_t \epsilon, \quad \epsilon \sim \mathcal{N}(0, I), \quad (1)$$

where α_t and σ_t are scheduling parameters that jointly determine the denoising ratio at each time step t according to different schedulers, such as DDPM (Ho et al., 2020) and Flow Matching (Kingma & Gao, 2024; Esser et al., 2024).

The denoising model ϵ_θ is trained to predict the noise ϵ added to x_t at each time step t by minimizing the discrepancy between the true noise and the model’s prediction. The loss function is defined as:

$$\mathcal{L}(\theta) = \mathbb{E}_{t, x_0, \epsilon} |\epsilon_\theta(x_t, t) - \epsilon|_2^2 \quad (2)$$

Latent Diffusion Models (LDMs) (Rombach et al., 2022) utilize Variational Autoencoders (VAEs) (van den Oord et al., 2017) to obtain low-dimensional latent representations, enabling more efficient diffusion processes. Similarly, in video generation, 3D-VAEs (Yu et al., 2023) compress both spatial and temporal dimensions of videos, simplifying the learning task for diffusion models. The denoising network ϵ_θ can be implemented using architectures such as U-Net or Diffusion Transformers.

4. CustomVideoX

4.1. 3D Reference Attention

In CogVideoX, the video and text interact through 3D Full Attention. The video input $X \in \mathbb{R}^{T \times H \times W \times C}$ is compressed into the latent space z_v via a 3D causal VAE (Yu et al., 2023). The text input T is processed through the T5 text encoder (Chung et al., 2022) to obtain z_t . Both z_v and z_t are encoded using their respective visual and text expert transformers, respectively. They then interact within the multi-modal attention mechanism (Esser et al., 2024) to

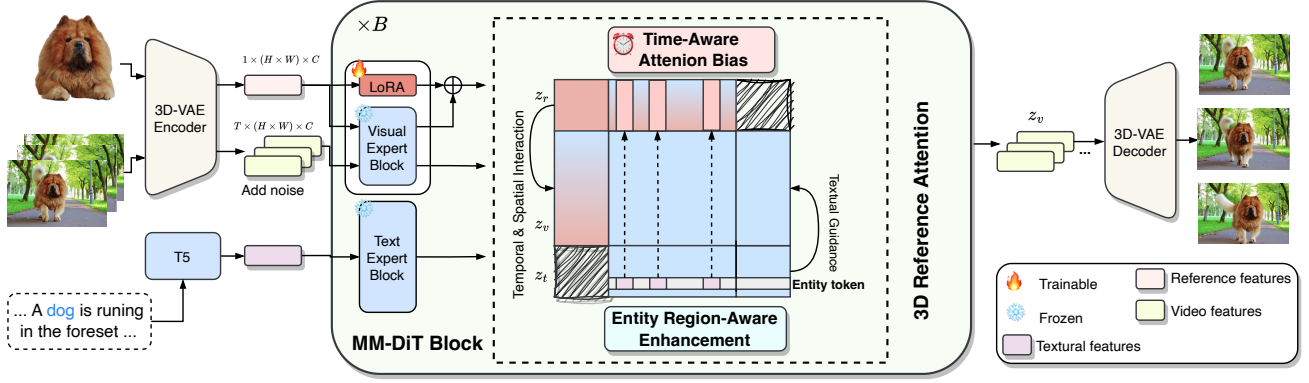


Figure 2: The overall pipeline of CustomVideoX. CustomVideoX is capable of producing personalized videos that conform to specified instructions, utilizing provided image objects and textual descriptions. It enhances each video frame by incorporating reference image through *3D Reference Attention* mechanism, allowing for dynamic interactions between the reference images and video frames, both temporally and spatially. Moreover, CustomVideoX employs a *Time-Aware Attention Bias* strategy and an *Entity Region-Aware Enhancement* module to boost spatial and temporal coherence throughout the denoising process, enabling the model to maintain consistent reference feature capture across frames.

produce the final output, as formulated as:

$$\begin{aligned} z_v &= \text{VisualExpert}(z_v), \quad z_t = \text{TextExpert}(z_t) \\ z_v, z_t &= \text{MM-Attention}(z_v, z_t) \end{aligned} \quad (3)$$

Prior methods (Ye et al., 2023; Hu et al., 2024) typically depend on auxiliary networks or adapters to inject reference image features, which often introduces misalignment with native video representations and necessitates costly retraining. To address this, as shown in Figure 2, we propose a parameter-efficient adaptation of the video expert transformer by integrating LoRA (Hu et al., 2021) to adapt these blocks for handling the additional reference image condition features without compromising the pre-trained model’s integrity.

Specifically, we encode the reference image using a 3D causal VAE to obtain z_r . The z_r is then processed through a vision expert transformer equipped with LoRA parameters for learnable training. Subsequently, we can naturally connect the z_r , z_v , and z_t to perform 3D Reference Attention mechanism, formulated as:

$$\begin{aligned} z &= \text{Concat}([z_v, z_t, z_r]), \\ z_{3D\text{-ref}} &= \text{Softmax}\left(\frac{(zW_Q)(zW_K)^\top}{\sqrt{d_k}}\right)(zW_V), \quad (4) \\ z_t, z_v, z_r &= \text{Split}(z_{3D\text{-ref}}), \end{aligned}$$

where Concat denotes the concatenate operation, Split indicates the split operation. W_Q , W_K , W_V are the learnable linear layer. Notably, in the 3D Reference Attention, the positional encoding of z_r is shifted:

$$p_r = p_v + \delta, \quad (5)$$

where p_v is the token position in z_v and the shift δ allows z_r to interact more effectively with z_v . 3D Reference Attention enables flexible token interactions, allowing direct relationships to emerge between any pair of tokens without imposing rigid spatial constraints.

4.2. Time-Aware Attention Bias

To harmonize pre-trained denoising capabilities with robust reference feature integration, we propose the Time-Aware Bias (TAB) mechanism, a phase-adaptive modulation strategy for cross-attention layers. TAB dynamically adjusts reference feature influence via a parabolic temporal mask, formalized as:

$$\tilde{A}_{ref} = \text{Softmax}\left(\frac{QK_{ref}^\top}{\sqrt{d}} + \tanh(M(t))\right)V_{ref}, \quad (6)$$

where $Q = zW_Q$, $K_{ref} = z_{ref}W_K$, and $V_{ref} = z_{ref}W_V$, the temporal modulation function $M(t)$ adopts an inverted parabolic profile:

$$M(t) = -\gamma\left(\frac{2t}{T} - 1\right)^2 + \epsilon. \quad (7)$$

Here, $t \in [0, T]$ indexes the denoising timestep, $\gamma = 10$ (empirically determined) governs suppression intensity, and $\epsilon = 0.1$ ensures numerical stability. As illustrated in Figure 3, the U-shaped design of $M(t)$ achieves three synergistic objectives: **Boundary Suppression** strategically attenuates reference feature influence at $t = 0$ and $t = T$ through parabolic minima, preserving structural fidelity by leveraging pre-trained denoising priors during critical initialization and finalization phases; **Mid-phase Enhancement** emerges via neutral bias conditions ($M(t) \approx 0$) around $t = T/2$,

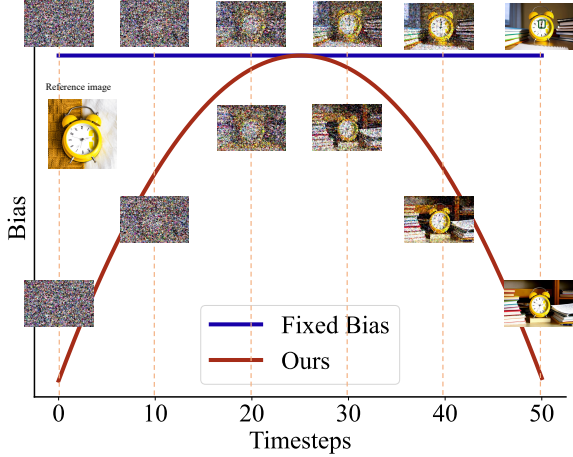


Figure 3: The time-aware attention bias v.s. fixed attention bias in the sampling process. TAB dynamically regulates the influence of reference features using a parabolic temporal mask, enhancing the consistency of reference images throughout the generation sequence.

allowing full assimilation of reference features during the intermediate refinement stage; while **Progressive Transition** is mathematically guaranteed by the C^2 -continuous parabolic profile, ensuring differentiable temporal evolution that maintains gradient stability throughout the denoising trajectory. This temporally modulated architecture enables phase-specific feature emphasis without compromising the backbone model’s inherent generative capabilities.

4.3. Entity Region-Aware Enhancement

Conventional approaches for principal content emphasis often employ explicit mask-guided paradigms to constrain video generation to key image regions, at the cost of sacrificing output diversity. To resolve this fundamental trade-off, we propose the **Entity Region-Aware Enhancement (ERAE)** module, which achieves adaptive region emphasis through latent semantic alignment without hard spatial constraints. Given a semantic entity token (e.g., “dog”), the module computes coarse entity regions via activation thresholding:

$$\begin{aligned} R_e &= \mathbb{I}(A_e > \lambda), \\ A_r &\leftarrow A_r + b_1 \odot R_e, \end{aligned} \quad (8)$$

where $\mathbb{I}(\cdot)$ denotes the indicator function, $A_e \in \mathbb{R}^{H \times W}$ represents activation intensity from cross-modal attention, and $\lambda = 0.1$ serves as the empirically determined intensity threshold. The target feature map A_r receives localized reinforcement through element-wise multiplication (\odot) with enhancement magnitude $b_1 = 0.1$, calibrated to preserve background generation flexibility.

This formulation induces two complementary effects: (i) *semantic grounding* through gradient-aware amplification

Algorithm 1 CustomVideoX Generation Pipeline

- 1: **INPUT:** Pre-trained video diffusion model \mathcal{M}_θ , LoRA-parameterized variant \mathcal{M}_{θ_L} , reference image $\mathbf{x}_{\text{ref}} \in \mathbb{R}^{H \times W \times 3}$, entity tokens \mathcal{E} , total timesteps T
- 2: **INIT:** Sample $\mathbf{z}_v^{(T)} \sim \mathcal{N}(0, \mathbf{I})$, initialize hyperparameters: $\{\lambda = 0.1, \beta_1 = 0.1, \gamma = 10, \epsilon = 0.1\}$
- 3: Extract reference features $\mathbf{z}_{\text{ref}} \leftarrow \mathcal{M}_{\theta_L}(\mathbf{x}_{\text{ref}})$
- 4: **for** $t = T$ to 0 **do**
- 5: Compute time-aware attention bias M_t \triangleright Eq. (7)
- 6: Generate entity region mask R_e \triangleright Eq. (8)
- 7: Update latent state via reference-attention:

$$\mathbf{z}_v^{(t-1)} \leftarrow \mathcal{M}_\theta(\mathbf{z}_v^{(t)}, t, M_t \odot R_e, \mathbf{z}_{\text{ref}})$$

\triangleright Eq. (4)

8: **end for**

9: **Output:** Generated video $\mathbf{v} = \mathcal{D}(\mathbf{z}_v^{(0)})$ $\triangleright \mathcal{D}$: decoder

of entity-associated activations, and (ii) *context preservation* via controlled magnitude modulation. As demonstrated in Algorithm 1, the differentiable thresholding operation enables end-to-end learning of region-semantic correspondence.

5. Dataset

5.1. Training Video Dataset

Despite the abundance of datasets for customized image generation, resources for customized video generation remain limited. In this study, we introduce a high-quality, customized single-object dataset tailored for training purposes. We curated aesthetically appealing data from the open-source OpenVid dataset. Using Grounding-DINO (Liu et al., 2023) and SAM (Kirillov et al., 2023) for annotation, we extracted objects from selected frames to serve as references, with the subsequent N frames used as ground truth. Overall, we have amassed a collection of 51K data samples. The dataset encompasses a diverse range of sources including humans, animals, vehicles, buildings, and natural scenes. As detailed in Appendix A, all data undergoes rigorous quality control through a three-stage validation process incorporating video resolution, aesthetic score, motion score and temporal consistency checks.

5.2. VideoBench Benchmark

To assess the performance of customized video generation, we have developed a benchmark, **VideoBench**, depicted in Figure 4. This benchmark comprises video generation tasks for 50 different objects and over 100 prompts, ensuring no overlap with the training set.



Figure 4: Overview of the Proposed VideoBench Framework. From left to right, panel left illustrates word counting, while panel right provides visual examples demonstrating the application of the framework.

Table 1: Quantitative comparison of different methods across DreamBench and VideoBench benchmarks. **Bold** represents the best result and data underline represents the second-best result.

Methods	DreamBench					VideoBench				
	CLIP-T	CLIP-I	DINO-I	T.Cons	D.D	CLIP-T	CLIP-I	DINO-I	T.Cons	D.D
BLIP-Diffusion (Li et al., 2023)	29.97	<u>84.39</u>	84.14	95.87	54.87	29.85	88.83	87.99	96.88	36.00
IP-Adapter (Ye et al., 2023)	28.87	82.00	82.18	95.16	<u>56.64</u>	29.38	86.92	87.87	96.23	42.00
λ -Eclipse (Patel et al., 2024)	<u>34.01</u>	82.92	84.10	95.98	59.29	32.25	89.45	89.94	97.54	38.00
SSR-Encoder (Zhang et al., 2024)	29.32	83.24	83.92	95.42	59.29	29.97	87.01	87.74	96.63	40.00
MS-Diffusion (Wang et al., 2024)	33.74	85.47	<u>87.54</u>	<u>96.65</u>	53.98	<u>32.64</u>	90.55	<u>91.29</u>	<u>97.35</u>	54.00
VideoBooth (Jiang et al., 2024)	28.99	76.42	77.90	96.17	45.13	28.92	82.60	84.06	96.75	<u>46.00</u>
CustomVideoX (Ours)	34.28	85.47	88.17	96.77	50.44	33.38	<u>90.26</u>	91.49	97.26	<u>46.00</u>

6. Experiments

6.1. Experimental Setup

Implementation Details. We use CogVideoX-5B as our base model and apply LoRA (Hu et al., 2021) to fine-tuning, setting the rank to 128. This approach introduces only an additional 2.3% of trainable parameters, thereby reducing training complexity while maintaining model performance. All experiments are carried out on 16 NVIDIA H20 GPUs, with a batch size of 1 per GPU and gradient accumulation set to 2. During training and inference, the resolution of the frame is fixed at 480×720 pixels, and 25 sequential frames are extracted per video at an interval of three frames. For optimization, we employ the AdamW optimizer with a fixed learning rate of $1e-5$ and a weight decay of $1e-2$. The model is trained for a total of 10,000 steps. Regarding hyperparameters, we define and utilize a Time-Aware Initialization Attention mechanism to enhance the model’s temporal awareness. During inference, we use DDIM (Song et al., 2020) with 50 inference steps to generate videos.

Evaluation Metrics. Following (Jiang et al., 2024; Wu et al., 2024a), we evaluate the quality of the generated videos from two perspectives: overall consistency and subject fidelity. For overall consistency, we employ three metrics: CLIP-T, Temporal Consistency (T.Cons), and Dynamic De-

gree (D.D). CLIP-T measures the average cosine similarity between the CLIP (Radford et al., 2021) image embeddings of all generated frames and their corresponding text embeddings. T.Cons calculates the average cosine similarity between the CLIP image embeddings of consecutive frames, assessing temporal coherence. D.D (Huang et al., 2024) utilizes optical flow to quantify motion dynamics within the video. To evaluate subject fidelity, we use CLIP-I and DINO-I for both customized human and object video generation tasks. CLIP-I assesses the visual similarity between the generated frames and the target subjects by computing the average cosine similarity between the CLIP image embeddings of all generated frames and the reference images. DINO-I (Caron et al., 2021) is another metric of visual similarity, utilizing the ViT-S/16 model.

Comparison Methods. We combine several customized image generation approaches, i.e., BLIP-Diffusion (Li et al., 2023), IP-Adapter (Ye et al., 2023), λ -Eclipse (Patel et al., 2024), SSR-Encoder (Zhang et al., 2024), MS-Diffusion (Wang et al., 2024), with the Cogvideox5b-I2V (Yang et al., 2024) model (image-to-video) to develop a naive two-stage customized video generation pipeline for comparison with our proposed method. Additionally, we compared our approach with the fine-tuning-based model VideoBooth (Jiang et al., 2024).

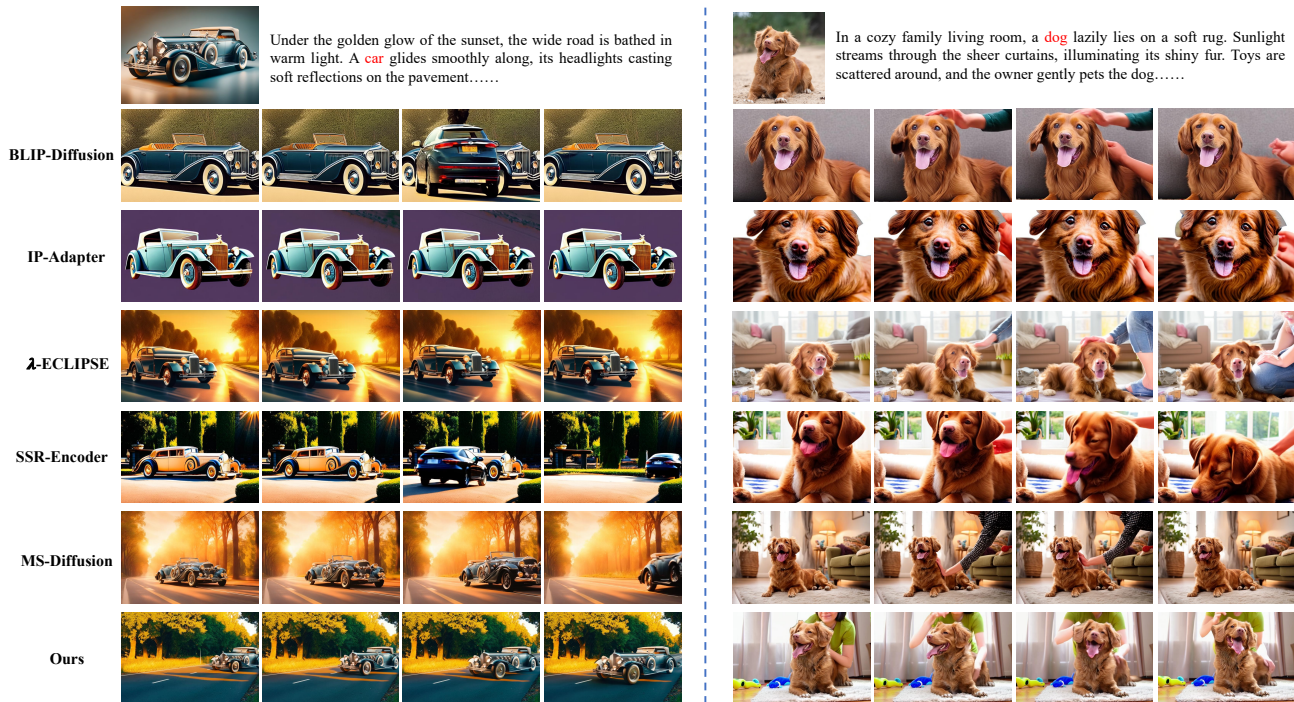


Figure 5: The qualitative results compared to the personalized model (+ I2V model). When compared to several different methods, CustomVideoX clearly demonstrates superior capabilities on concept fidelity and caption semantic consistency



Figure 6: Compared with VideoBooth. CustomVideoX adopts the optimal solution to effectively preserve the fidelity of image prompts and achieve better visual quality.

6.2. Quantitative Comparison

We evaluated the proposed method using two benchmarks: DreamBench and VideoBench. The quantitative results are illustrated in Table 1. Compared to the naive custom video generation approach, our model demonstrates comprehensive superiority across two different benchmarks. Specifically, in terms of text alignment, our approach outperforms the second-place method, ms-diffusion, by an average of 0.52%. Regarding subject fidelity, our method exceeds the second-place approach by 1.37% in CLIP-I and 1.72% in DINO-I, highlighting our model’s exceptional capability in maintaining consistency. In terms of video generation quality, our approach also achieves the best results in T.Cons. **Although it performs slightly weaker in D.D compared to other methods, this is because the CogvideoX-5b I2V model tends to generate incoherent cases with large inter-frame variations.** While the motion scale is higher, coherence is compromised, as corroborated by the T.Cons scores. Compared to the finetune-based customized video generation approach VideoBooth, our method significantly outperforms VideoBooth in all aspects, confirming the robust capabilities of our approach in concept fidelity and video quality.

Qualitative Comparison. In Figure 5, we present a comparative analysis between our proposed method and the naive customized video generation approach. In the first sample,

Table 2: **Impacts of different modules.** We refer to *A* as the 3D-Reference-Attention module, *B* as the TAB module, and *C* as ERAE. **Bold** represents the best result and data underline represents the second-best result.

<i>A</i>	<i>B</i>	<i>C</i>	CLIP-T	CLIP-I	DINO-I	T.Cons	DD
			27.31	74.45	76.57	95.45	38.00
✓			<u>33.56</u>	89.89	<u>91.13</u>	97.29	42.00
✓	✓		33.86	<u>90.10</u>	91.12	97.24	<u>44.00</u>
✓	✓	✓	33.38	90.26	91.49	<u>97.26</u>	46.00

which depicts a vehicle in motion, our method significantly outperforms the naive methods in terms of subject fidelity. Furthermore, both BLIP-Diffusion and SSR-Encoder exhibit instances where an additional car passes by in the video, a limitation inherent to naive customized video generation. This issue arises because I2V models struggle to bind subjects in the image with their corresponding concepts in the text, leading to the generation of extraneous subjects. Similarly, in the second sample, which features a dog interacting with its owner, our method achieves the best results in both subject fidelity and text alignment. Figure 6 illustrates a comprehensive visual comparison between our proposed method and Videobooth. In the first example, which involves generating a robot toy, our method demonstrates superior performance in subject fidelity compared to Videobooth. Furthermore, our approach ensures consistent identity preservation of the robot during motion, effectively avoiding distortions and structural collapses. In the second example, depicting a "panda munching on bamboo shoots," Videobooth, although maintaining some level of subject fidelity, fails to accurately capture the "munching" action. In contrast, our method successfully executes this instruction, achieving both action accuracy and naturalness.

6.3. Ablation Studies

To validate the effectiveness of the proposed components, we conduct comprehensive ablation studies. The quantitative results are presented in Table 2, while the qualitative results are shown in Figure 7.

Naive Reference Image Injection. In this baseline approach, the reference target image is simply injected as an additional frame input to the model. As illustrated in the first column of Figure 7, this method struggles to maintain object consistency across the generated video, resulting in noticeable fluctuations in the target’s appearance throughout the sequence.

3D Reference Attention Injection. The 3D Reference Attention injection method introduced in this paper demonstrates significant improvements across all evaluation metrics. Notably, the CLIP-I and DINO-I scores increased by 15.44% and 14.56%, respectively, particularly improving



Figure 7: Ablation study visualizations comparing module contributions. Demonstration of the effectiveness of the 3D Reference Attention, TAB, and ERAE modules.

target consistency. The proposed shift position encoding addresses the issue of high consistency between the initial frame and the reference target while ensuring sustained consistency in subsequent frames. By enabling each frame of the video to focus equally on the reference object, shift position encoding enhances the ability to generate consistent targets.

Time-Aware Attention Bias. The proposed Time-Aware Attention Bias employs a progressive reference information injection approach, providing the model with a more stable learning process during the initial stages. This method further improves target consistency upon completion.

Entity Region-Aware Enhancement. Entity Region-Aware Enhancement adaptively applies additional interactions to highly correlated tokens within the video based on the target text tokens. This approach not only improves target consistency in video generation but also enhances the interaction between the target and the environment, increasing the dynamic quality of the video. As indicated by the D.D metric in Table 2, the absence of this module results in a reduction of 2. Notably, our training dataset does not include clothing categories, highlighting the strong generalization capability of CustomVideoX.

7. Conclusions

In this paper, we present CustomVideoX, a zero-shot model for customized video generation. CustomVideoX extracts reference image information through a single network and injects the reference features into the noise using region-

aware and time-aware feature adjustments. This enables convenient and continuous extraction of reference features. Additionally, the model leverages 3D reference attention, allowing for natural interaction between the reference object and each frame of the generated video. To train and evaluate CustomVideoX, we have collected a high-quality customized video dataset. Experimental results demonstrate that CustomVideoX achieves state-of-the-art performance on DreamBench and VideoBench.

Impact Statement

This paper presents work that aims to advance the field of Machine Learning and Video Generation. There are many potential societal consequences of our work, none of which we feel must be specifically highlighted here.

References

- Betker, J., Goh, G., Jing, L., Brooks, T., Wang, J., Li, L., Ouyang, L., Zhuang, J., Lee, J., Guo, Y., et al. Improving image generation with better captions. *Computer Science*. <https://cdn.openai.com/papers/dall-e-3.pdf>, 2:3, 2023.
- Caron, M., Touvron, H., Misra, I., Jégou, H., Mairal, J., Bojanowski, P., and Joulin, A. Emerging properties in self-supervised vision transformers. In *ICCV*, 2021.
- Chefer, H., Zada, S., Paiss, R., Ephrat, A., Tov, O., Rubinstein, M., Wolf, L., Dekel, T., Michaeli, T., and Mosseri, I. Still-moving: Customized video generation without customized video data. *ACM Transactions on Graphics (TOG)*, 43(6):1–11, 2024.
- Chen, X., Huang, L., Liu, Y., Shen, Y., Zhao, D., and Zhao, H. Anydoor: Zero-shot object-level image customization. *CoRR*, abs/2307.09481, 2023.
- Chung, H. W., Hou, L., Longpre, S., Zoph, B., Tay, Y., Fedus, W., Li, Y., Wang, X., Dehghani, M., Brahma, S., et al. Scaling instruction-finetuned language models. *arXiv preprint arXiv:2210.11416*, 2022.
- Esser, P., Kulal, S., Blattmann, A., Entezari, R., Müller, J., Saini, H., Levi, Y., Lorenz, D., Sauer, A., Boesel, F., et al. Scaling rectified flow transformers for high-resolution image synthesis. In *ICML*, 2024.
- Gal, R., Alaluf, Y., Atzmon, Y., Patashnik, O., Bermano, A. H., Chechik, G., and Cohen-Or, D. An image is worth one word: Personalizing text-to-image generation using textual inversion. In *ICLR*, 2023.
- Guo, Y., Yang, C., Rao, A., Wang, Y., Qiao, Y., Lin, D., and Dai, B. Animatediff: Animate your personalized text-to-image diffusion models without specific tuning. In *ICLR*, 2024.
- He, W., Fu, S., Liu, M., Wang, X., Xiao, W., Shu, F., Wang, Y., Zhang, L., Yu, Z., Li, H., et al. Mars: Mixture of auto-regressive models for fine-grained text-to-image synthesis. In *AAAI*, 2025.
- Ho, J., Jain, A., and Abbeel, P. Denoising diffusion probabilistic models. In *NeurIPS*, 2020.
- Ho, J., Salimans, T., Gritsenko, A., Chan, W., Norouzi, M., and Fleet, D. J. Video diffusion models. In *NeurIPS*, 2022.
- Hu, E. J., Shen, Y., Wallis, P., Allen-Zhu, Z., Li, Y., Wang, S., Wang, L., and Chen, W. Lora: Low-rank adaptation of large language models. In *ICLR*, 2021.
- Hu, L., Gao, X., Zhang, P., Sun, K., Zhang, B., and Bo, L. Animate anyone: Consistent and controllable image-to-video synthesis for character animation. *arXiv*, 2024.
- Huang, Z., He, Y., Yu, J., Zhang, F., Si, C., Jiang, Y., Zhang, Y., Wu, T., Jin, Q., Chanpaisit, N., et al. Vbench: Comprehensive benchmark suite for video generative models. In *CVPR*, pp. 21807–21818, 2024.
- Hui, B., Yang, J., Cui, Z., Yang, J., Liu, D., Zhang, L., Liu, T., Zhang, J., Yu, B., Lu, K., et al. Qwen2. 5-coder technical report. *arXiv preprint arXiv:2409.12186*, 2024.
- Jiang, Y., Wu, T., Yang, S., Si, C., Lin, D., Qiao, Y., Loy, C. C., and Liu, Z. Videobooth: Diffusion-based video generation with image prompts. In *CVPR*, pp. 6689–6700, 2024.
- Kingma, D. and Gao, R. Understanding diffusion objectives as the elbo with simple data augmentation. In *NeurIPS*, volume 36, 2024.
- Kirillov, A., Mintun, E., Ravi, N., Mao, H., Rolland, C., Gustafson, L., Xiao, T., Whitehead, S., Berg, A. C., Lo, W.-Y., et al. Segment anything. In *ICCV*, pp. 4015–4026, 2023.
- Li, D., Li, J., and Hoi, S. C. H. Blip-diffusion: Pre-trained subject representation for controllable text-to-image generation and editing. In *NeurIPS*, 2023.
- Liu, M., Ma, Y., Zhen, Y., Dan, J., Yu, Y., Zhao, Z., Hu, Z., Liu, B., and Fan, C. Llm4gen: Leveraging semantic representation of llms for text-to-image generation. In *AAAI*, 2024.
- Liu, S., Zeng, Z., Ren, T., Li, F., Zhang, H., Yang, J., Li, C., Yang, J., Su, H., Zhu, J., et al. Grounding dino: Marrying dino with grounded pre-training for open-set object detection. *arXiv preprint arXiv:2303.05499*, 2023.

- Ma, J., Liang, J., Chen, C., and Lu, H. Subject-diffusion: Open domain personalized text-to-image generation without test-time fine-tuning. In *ACM SIGGRAPH*, pp. 1–12, 2024.
- Patel, M., Jung, S., Baral, C., and Yang, Y. *lambda*-eclipse: Multi-concept personalized text-to-image diffusion models by leveraging clip latent space. *arXiv preprint arXiv:2402.05195*, 2024.
- Peebles, W. and Xie, S. Scalable diffusion models with transformers. In *ICCV*, pp. 4172–4182, 2023.
- Podell, D., English, Z., Lacey, K., Blattmann, A., Dockhorn, T., Müller, J., Penna, J., and Rombach, R. SDXL: improving latent diffusion models for high-resolution image synthesis. *CoRR*, abs/2307.01952, 2023.
- Radford, A., Kim, J. W., Hallacy, C., Ramesh, A., Goh, G., Agarwal, S., Sastry, G., Askell, A., Mishkin, P., Clark, J., Krueger, G., and Sutskever, I. Learning transferable visual models from natural language supervision. In *ICML*, pp. 8748–8763, 2021.
- Rombach, R., Blattmann, A., Lorenz, D., Esser, P., and Ommer, B. High-resolution image synthesis with latent diffusion models. In *CVPR*, pp. 10674–10685, 2022.
- Ruiz, N., Li, Y., Jampani, V., Pritch, Y., Rubinstein, M., and Aberman, K. Dreambooth: Fine tuning text-to-image diffusion models for subject-driven generation. In *CVPR*, pp. 22500–22510, 2023.
- Song, J., Meng, C., and Ermon, S. Denoising diffusion implicit models. *arXiv preprint arXiv:2010.02502*, 2020.
- Sun, W., Cui, B., Tang, J., and Dong, X.-M. Attentive eraser: Unleashing diffusion model’s object removal potential via self-attention redirection guidance. *arXiv preprint arXiv:2412.12974*, 2024.
- Tan, Z., Liu, S., Yang, X., Xue, Q., and Wang, X. Ominicontrol: Minimal and universal control for diffusion transformer. *arXiv preprint arXiv:2411.15098*, 2024.
- van den Oord, A., Vinyals, O., and Kavukcuoglu, K. Neural discrete representation learning. In *NeurIPS*, pp. 6306–6315, 2017.
- Wang, X., Fu, S., Huang, Q., He, W., and Jiang, H. Ms-diffusion: Multi-subject zero-shot image personalization with layout guidance. *arXiv*, 2024.
- Wei, Y., Zhang, S., Qing, Z., Yuan, H., Liu, Z., Liu, Y., Zhang, Y., Zhou, J., and Shan, H. Dreamvideo: Composing your dream videos with customized subject and motion. In *CVPR*, pp. 6537–6549, 2024a.
- Wei, Y., Zhang, S., Yuan, H., Wang, X., Qiu, H., Zhao, R., Feng, Y., Liu, F., Huang, Z., Ye, J., et al. Dreamvideo-2: Zero-shot subject-driven video customization with precise motion control. *arXiv preprint arXiv:2410.13830*, 2024b.
- Wu, J. Z., Ge, Y., Wang, X., Lei, W., Gu, Y., Hsu, W., Shan, Y., Qie, X., and Shou, M. Z. Tune-a-video: One-shot tuning of image diffusion models for text-to-video generation. In *CVPR*, 2023.
- Wu, T., Zhang, Y., Cun, X., Qi, Z., Pu, J., Dou, H., Zheng, G., Shan, Y., and Li, X. Videomaker: Zero-shot customized video generation with the inherent force of video diffusion models. *arXiv preprint arXiv:2412.19645*, 2024a.
- Wu, T., Zhang, Y., Wang, X., Zhou, X., Zheng, G., Qi, Z., Shan, Y., and Li, X. Customcrafter: Customized video generation with preserving motion and concept composition abilities. *arXiv preprint arXiv:2408.13239*, 2024b.
- Yang, Z., Teng, J., Zheng, W., Ding, M., Huang, S., Xu, J., Yang, Y., Hong, W., Zhang, X., Feng, G., et al. Cogvideox: Text-to-video diffusion models with an expert transformer. *arXiv preprint arXiv:2408.06072*, 2024.
- Ye, H., Zhang, J., Liu, S., Han, X., and Yang, W. Ip-adapter: Text compatible image prompt adapter for text-to-image diffusion models. *arXiv preprint arXiv:2308.06721*, 2023.
- Ying, J., Liu, M., Wu, Z., Zhang, R., Yu, Z., Fu, S., Cao, S.-Y., Wu, C., Yu, Y., and Shen, H.-L. Restorerid: Towards tuning-free face restoration with id preservation. *arXiv preprint arXiv:2411.14125*, 2024.
- Yu, L., Lezama, J., Gundavarapu, N. B., Versari, L., Sohn, K., Minnen, D., Cheng, Y., Birodkar, V., Gupta, A., Gu, X., et al. Language model beats diffusion—tokenizer is key to visual generation. *arXiv preprint arXiv:2310.05737*, 2023.
- Zhang, Y., Song, Y., Liu, J., Wang, R., Yu, J., Tang, H., Li, H., Tang, X., Hu, Y., Pan, H., et al. Ssr-encoder: Encoding selective subject representation for subject-driven generation. In *CVPR*, pp. 8069–8078, 2024.
- Zhao, Z., Tang, J., Wu, B., Lin, C., Wei, S., Liu, H., Tan, X., Zhang, Z., Huang, C., and Xie, Y. Harmonizing visual text comprehension and generation. *arXiv preprint arXiv:2407.16364*, 2024.

A. Data Details

Figure 8 illustrates the pipeline for constructing our training data. In the first stage, we perform high-quality video data filtering. Firstly, we exclude videos with a resolution below 1080P to ensure high-definition video quality and clear subjects. Next, we apply a video aesthetic filter, removing videos with aesthetic scores below 5.3 to maintain aesthetic standards. Subsequently, we eliminate static or low-motion videos by evaluating motion scores and temporal consistency, discarding videos with poor temporal coherence.

In the second stage, for the filtered high-quality video data, we use Qwen2.5 (Hui et al., 2024) to extract the main entity from the video captions and assess the complexity of the video backgrounds based on these captions. This allows us to further remove data with redundant or complex backgrounds, ensuring that the videos contain a limited number of clear subjects with simple backgrounds. Finally, based on the extracted main entity, we utilize Grounding SAM to segment the first frame of the video, extract the corresponding objects, and create training pairs.

B. Implementation Details of CustomVideoX

With a LoRA rank of 128, CustomVideoX introduces 132.12M trainable parameters, accounting for only 2.3% of the total parameters of the model. In contrast, VideoBooth fine-tunes certain model parameters, resulting in 97.63M trainable parameters, which represent 8.8% of the total. Additionally, because VideoBooth modifies the base model, it inevitably leads to a reduction in video generation quality.

C. More Experimental Results

More results can be found in Figure 9 and Figure 10.

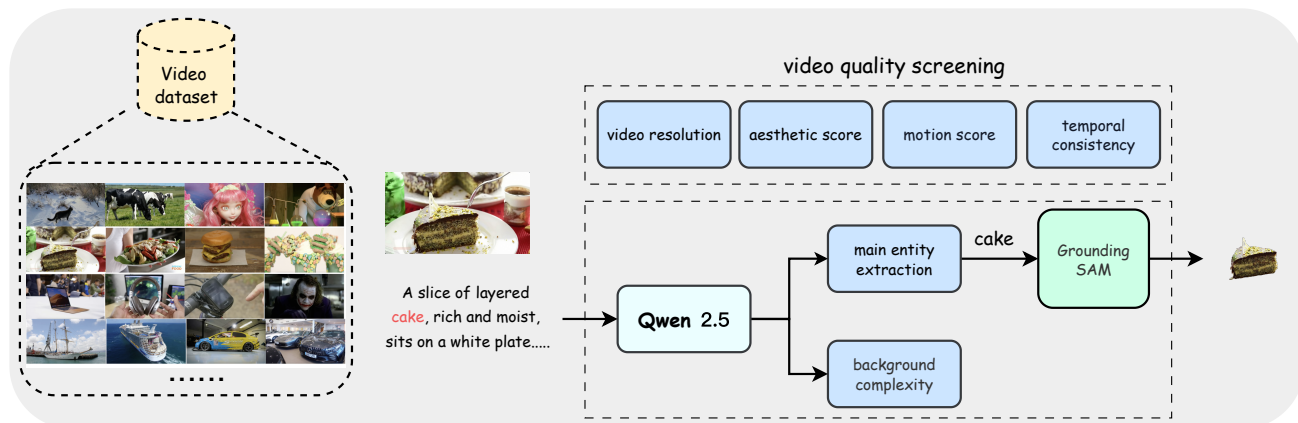


Figure 8: The overview of video customization data collection pipeline. When dealing with complex scenarios that contain concepts with Qwen2.5 and Grounding SAM models. Our data pipeline could still extract precise video quality via video resolution, aesthetic score, motion score, and temporal consistency.

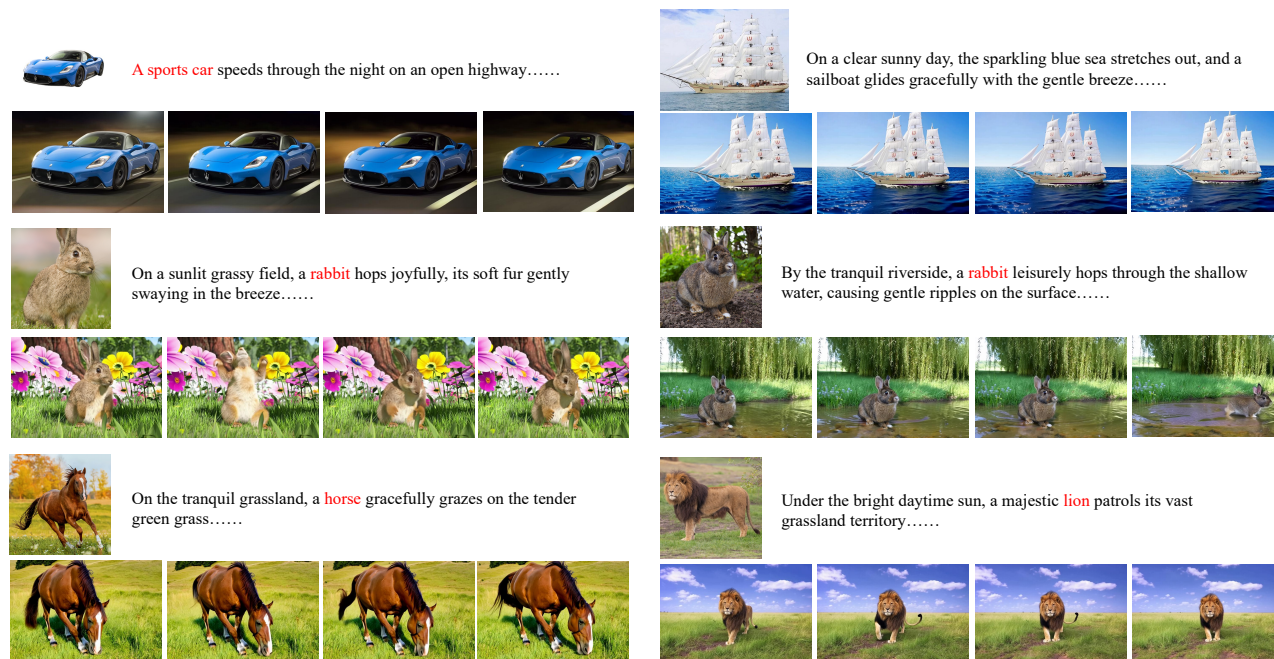


Figure 9: Additional results of subject personalization for video generation on diverse scenarios (1/2).

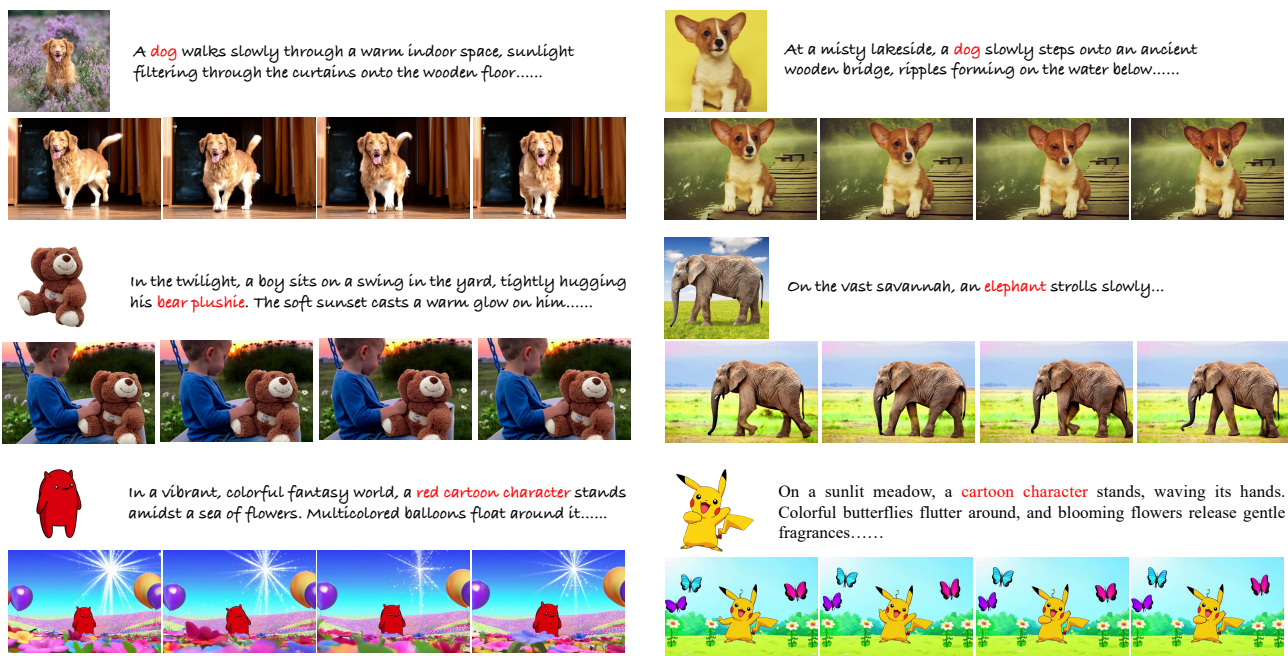


Figure 10: Additional results of subject personalization for video generation on diverse scenarios (2/2).